32nd URSI GASS, Montreal, 19–26 August 2017

Comparison of Recent Stimulated Electromagnetic Emission Observations at HAARP and EISACT

Haiyang Fu*(1), Wayne A. Scales(2), Paul A. Bernhardt(3), Stanley J. Briczinski(3)
(1) Fudan University, Shanghai, China
(2) Virginia Tech, Blacksburg, USA
(3) Naval Research Laboratory, DC, USA

Abstract

We compare observations of stimulated electromagnetic emission (SEE) during ionospheric modification experiments using ground-based high-power high-frequency (HF) radio waves at both the High Frequency Active Auroral Research Program (HAARP) and the European Incoherent scatter (EISCAT). The combined simultaneous observations of SEEs, field-aligned irregularities and electron temperature provides evidence that it is more efficient for electron temperature enhancement and plasma irregularity generation at frequency slightly above the third electron gyro-harmonic $3f_{\text{ce}}$. This study shows the utility of utilizing SEE, SuperDARN HF radar and UHF incoherent radar simultaneously to investigate electron heating mechanisms during ionospheric modification experiments.

1 Introduction

The interaction between high-power electromagnetic waves and plasmas in the ionosphere can produce stimulated electromagnetic emissions (SEEs), first reported by Thidé et al. [1] and reviewed by Leyser [2]. Stimulated electromagnetic emission (SEE) spectral lines in the scattered wave can be utilized to remotely probe the properties of the ionosphere as well as actively study radio pump-induced phenomenon such as artificial airglow during modification of the ionosphere [3, 4]. Historically, wide-band SEEs within ~ 100 kHz of the pump frequency, have been studied extensively for several decades at EISCAT. Due to updates of the HAARP facility in 2007, new SEE spectral lines have been observed at HAARP, including stimulated Brillouin scattering(SBS), stimulated ion Bernstein scattering (SIBS) and broad downshifted emission [5, 6, 7, 8, 9]. These new spectral lines exist within a narrow frequency band of the pump wave. For example, SBS during electron gyro-harmonic heating is well within 100 Hz of the pump frequency at EISCAT [10].

The EISCAT (69.6°N, 19.2°E) and HAARP (62.4°N, 145.2°W) HF heating facilities are located at high latitudes with a comparable geomagnetic angle. The EISCAT HF heater has approximately one third the power of the HARRP HF heater and only higher gyro-harmonic ($n \geq 3$) heating capability is available at EISCAT. Two HF heating facilities are both equipped with HF SuperDARN radars for field-aligned irregularities (FAIs) measurement. The EISCAT facility has an advantage of the EISCAT/UHF incoherent scatter radars for electron temperature measurement. The systematic comparison of SEEs at two heating facilities is lacking and the correlation between SEEs, FAIs and electron temperature has not been well understood. The paper summarizes SEE observations with simultaneous measurement of field-aligned irregularities and electron temperature during ionospheric modification experiments at HAARP and EISCAT near electron gyro-harmonic $3f_{\text{ce}}$.

2 Narrow-band SEEs and Field-aligned Irregularities

The experiment at HAARP was conducted on July 18 $\sim$ 23, 2010 with the HF transmitter operating at O-mode polarization with an effective radiated power (ERP) of 1.0 gigawatts for the pump frequency 4.5 MHz. The pump frequency f_0 was selected near the third electron gyro-harmonic (4.1 MHz $\leq$ f$_0$ $\leq$ 4.3MHz) for varying beam zenith angles ZA. The magnetic zenith corresponds to ZA $= 14^{\circ}$ with the azimuth angle AZ $= 202^{\circ}$. The experiment at EISCAT was conducted on July 3-10, 2012 with the HF transmitter operating at O-mode polarization with full power. The pump frequency was in a range 3.9 MHz $\leq$ f$_0$ $\leq$ 4.2 MHz through the third harmonic of the ionospheric electron gyro-frequency $3f_{\text{ce}}$. All 12 transmitters on array 2 were used at 80kW each, resulting in a gain of 22.4 dBi and the effective radiated power (ERP) approximately 148 MW. The beam zenith angle was pointing along the magnetic field line (ZA $= 12^{\circ}$).

Figure 1 depicts the side-band frequency spectra of scattered electromagnetic waves (a) from the HAARP transmitter at 4.1 MHz for varying zenith beams and (b) for the EISCAT HF transmitter at 4.02 MHz at the magnetic zenith. In Figure 1a, the first spectral line f_1 downshifted by 8 $\sim$ 11Hz, are observed with power within 10 dB relative to the reflected pump wave. The upshifted emission lines with lower intensity has slightly higher 3 $\sim$ 4 Hz frequency offset than the downshifted emission lines due to interactions between reflected pump and scattered EM waves [4]. The power of the downshifted (or Stokes) emission line is larger than the upshifted (anti-Stokes) emission.

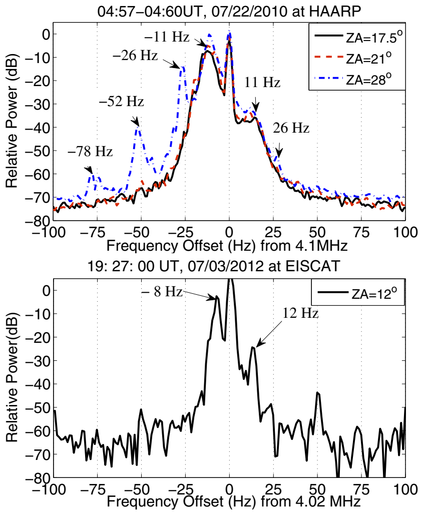

Figure 1. Measured frequency spectra of radio emissions (a) from the HAARP transmitter at 4.1MHz and (b) for EISCAT transmitter at 4.02MHz near $3f_{ce}$.

These spectral lines $f_1 = 8 \sim 11$Hz are considered to be associated with ion acoustic waves due to SBS from the plasma resonance region. Experimental results at EISCAT indicate that SBS strengthens as the pump frequency approaches to $3f_{ce}$ [9]. It is postulated that when less anomalous absorption occurs near $3f_{ce}$, and field-aligned irregularities FAIs and electron temperature enhancement shows its minimum as shown in Figure 2, more heater power can be transmitted to a higher resonance altitude where SBS occurs. Emissions at approximately ~ 26Hz were occasionally observed and may result from SBS from the upper hybrid resonance altitude. Further experiments are required to compare electron temperature with UHF incoherent scatter radar measurements.

Figure 2 depicts the electron temperature profile measured by the EISCAT UHF radar during $18:40-19:38$ UT on July 3, 2012. The pump frequency is stepped upwards and downwards between 3.92MHz $\sim$ 4.2MHz, respectively. For the upward frequency stepping, the electron temperature enhancement minimizes during $18:54-18:55$ ($f_0 = 4.06$MHz) and $18:56-18:57$($f_0 = 4.08$MHz) and the CUTLASS backscatter power (not shown here) decreases as well [11]. For the downward frequency stepping, the electron temperature enhancement reduces during $19:22-19:23$ ($f_0 = 4.06$MHz) and $19:24-19:25$ ($f_0 = 4.04$MHz), which corresponds to strong SBS emissions. The electron temperature enhancement minimizes when the pump frequency approaches $3f_{ce}$. The electron temperature enhancement exhibits an asymmetry for pump frequencies above and below $3f_{ce}$ in Figure 2. It should be noted that the measurement error increases during $19:08-19:15$ for $f_0 > 3f_{ce}$ in the narrow altitude range close to the heater reflection height since the electron temperature retrieval algorithm is based on the ion-line spectra which are modified by HF pump induced effects. It may indicate that there is higher electron temperature enhancement or plasma irregularities may be produced and involved in electron heating for $f_0 > 3f_{ce}$.

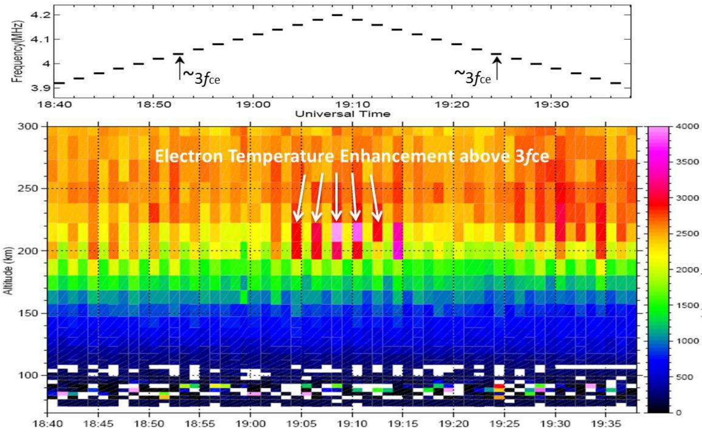

Figure 2. The electron temperature measured by the EISCAT UHF radar during 18:40-19:40 UT on July 3, 2012.

3 Temporal Evolution of Field-aligned Irregularities with SEEs

The experiment conducted on August 6, 2012 at HAARP provides wide-band SEE temporal evolution with simultaneous measurement of field-aligned irregularities by SuperDARN Kodiak radars. The polarization of SEE spectral components is also analyzed which reflects the randomness of plasma irregularities. The pump frequency was swept from 4.2MHz to reach 4.4MHz within 3 minutes. The spectrogram here is obtained by taking a Fourier Transform on the received signals with a Blackman window based on the North-South channel antenna signal. The spectrogram of received signals exhibits similar results from the N-S channel and W-E channel at Riverview and Tonsina Rivers sites, respectively. The time history of the field component E_{NS} from the N-S channel and E_{WE} from the W-E channel are synchronized based on the correlation technique for the maximum overshoot amplitude when the transmitter is turned on.

Figure 3 shows the time evolution of wide-band SEE features from the Riverview site (left) and SuperDARN Kodiak backscatter radar echoes (right) when pumping near $3f_{ce}$ for zenith angle 18^o during the time interval 4:29 - 4:32 on August 6, 2012. Classical SEE spectral lines are observed, including the downshifted maximum (DM) and its nth harmonic (nDM), the upshifted maximum (UM), and the broadband upshifted maximum (BUM) and its harmonic (nBUM). The time evolution of each SEE spectral component is clearly distinguishable and described as following. For f_0 starting from 4.2MHz at $t \sim 0$s , the DM at $f_{DM} = -(8 \sim 9\text{kHz})$ and its harmonics nDM are observed. For $f_0 \simeq 4.254 \sim 4.2605$MHz at time $48 \sim 54$s, we first observed downshifted and upshifted emissions with

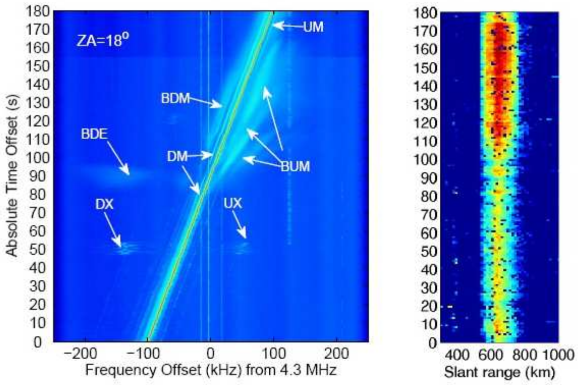

Figure 3. Frequency spectra of radio emissions from the HAARP transmitter (left) and SuperDARN kodiak backscatter radar echoes (right) during 04:29:00-04:32:00 UT on August 6, 2012.

frequency offset at ~ 75 kHz. These SEE emissions are newly observed, which are a downshifted emission labeled as DX and an upshifted emission labeled as UX. As f_0 approaches 4.294 MHz $\sim$ 4.304 MHz at time 85 $\sim$ 94 s, a broadband downshifted emission BDE occurs and spans a wide frequency band from 50 $\sim$ 180 kHz approximately peaked at $\sim$ 150 kHz . As f_0 increases to 4.304 MHz, the BDE damps out while the DM spectra narrows. The BDE emission occurs for the pump frequency $\sim$ 10 kHz well below $3f_{\mathrm{ce}}$. These BDE observations agree well with observations for beam towards the magnetic zenith [8]. Afterwards, the DM amplitude immediately reaches its minimum at time $t \sim 95$ s, indicating the third electron gyro-harmonic $f_0 \sim 3f_{\mathrm{ce}} \simeq 4.305$ MHz. As f_0 increases from slightly below to above $3f_{\mathrm{ce}}$, the BUM emission f_{BUM} and its harmonic $2f_{\mathrm{BUM}}$, $3f_{\mathrm{BUM}}$ starts to develop. The BUM develops at the onset time $t \simeq 85$ s of the DM suppression and remains for pumping frequency $f = 4.30$ MHz $\sim$ 4.38 MHz at time $t = 85 \sim 165$ s. The BUM emission covers a wide frequency range $f_{\mathrm{BUM}} = 15$ kHz $\sim$ 100 kHz. At time $t = 100$ s, broad downshifted maximum f_{BDM} occurs with the mirror frequency of the f_{BUM} at $\sim$ 20 kHz. In the vicinity of the BUM disappearance, the UM emission starts to develop at later time $t \sim 150$ s.

The right column of Figure 3 shows the concurrent observations of field-aligned irregularities measured by SuperDARN Kodiak radar. The HF backscatter radar echoes clearly exhibits stronger enhancement for pumping above electron gyro-harmonic $f_0 > 3f_{\mathrm{ce}}$ than that for pumping below $f_0 < 3f_{\mathrm{ce}}$. The enhanced radar echoes increased in amplitude approximately at time $t \sim 100$ s, corresponding to the most prominent BUM features in SEE spectrum. This backscatter radar echo asymmetry becomes the most obvious for pumping close to the magnetic zenith for ZA $= 18^{\mathrm{o}}$.

It is noted that this asymmetry has also been observed to produce artificial descending layers for $f_0 > 4f_{\mathrm{ce}}$ with magnetic zenith pumping and airflow enhancement at 427.8 nm

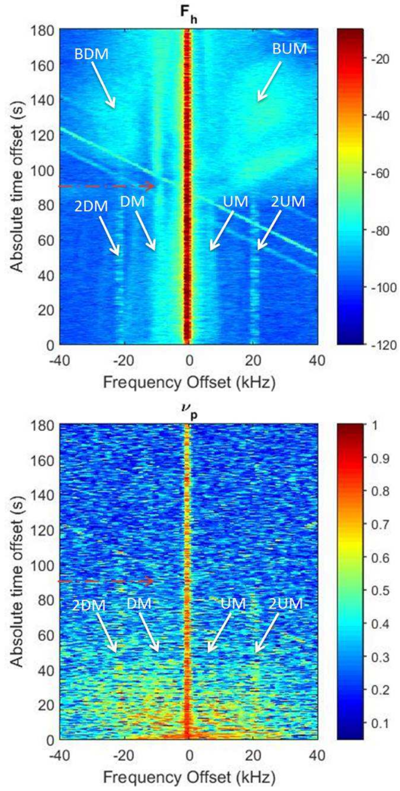

Figure 4. Spectrogram of the spectral intensity F_{h} and the degree of pure circular polarization v_p near $3f_{\mathrm{ce}}$ at HAARP during 04:29:00-04:32:00 on August 6, 2012.

from N_2^+ which require electrons with energies above the 18 eV ionization energy [3]. The temperature asymmetry has also been observed by UHF incoherent scatter radar near $3f_{\mathrm{ce}}$ at EISCAT in Figure 2. The correlation of the heating asymmetry between HAARP and EISCAT indicate that BUM generation involves field-aligned irregularities as well as high energy electron acceleration for pumping $f_0 > 3f_{\mathrm{ce}}$. Based on the theory [11], the BUM emissions, as a four-wave parametric decay process, are associated with field-aligned irregularities. The nonlinear evolution of BUM structures and coupling with field-aligned irregularities as a four-wave parametric decay instability is being pursued utilizing kinetic plasma simulation models and will be the subject of a future publication.

Figure 4 shows the spectrogram of the spectral intensity F_{h}, and the degree of pure circular polarization v_p near $3f_{\mathrm{ce}}$ for zenith angle 18^{o} at HAARP during $4:29-4:32$ on August 6, 2012. The definition of the spectral intensity F_{h} and v_p can be found according to [12]. As v_p approaches to 1, the polarization becomes circularly polarized. The maximum v_p value observed is above 75% circularly polarized at the frequency corresponding to the pump wave frequency. There are visible peaks of approximately 40% circularly polarized at the frequency corresponding to the DM, 2DM, UM and 2UM for time interval $0 < t < 85$ s. Otherwise, there is no clear v_p peak values since the spectrum is exhibited by BUM after $t > 85$s. The spinor tilt angle ϕ

spectrum (not shown) also exhibits an extremum at approximately 15^{o} relative to the N-S alignment, which matches the DM, 2DM, UM and 2UM frequency. There are no clear distinct polarization features for the BUM spectrum. Thus, it proves that when pumping above $3f_{\rm ce}$ for time $t > 85$s, plasma irregularities are expected to occur which depolarized the electromagnetic waves. The enhanced HF radar echoes indicated enhanced field-aligned irregularities for pumping above $3f_{\rm ce}$, but it cannot exclude that small-scale plasma irregularities may also exist with the BUM formation but cannot be sensitively measured by HF radars.

4 Conclusion

In summary, we compared the temporal evolution and correlation of narrow-band and wide-band SEEs with FAIs and electron temperature near $3f_{\rm ce}$ at EISCAT and HAARP. It is found that field-aligned irregularities are important for narrow-band and wide-band SEEs generation and propagation. It is demonstrated for the first time that HF backscatter radar echoes and electron temperature exhibits clear asymmetry for pumping above $3f_{\rm ce}$ than pumping below $3f_{\rm ce}$. By incorporating the SEE polarization analysis, it is shown to be plausible that for pumping above $3f_{\rm ce}$, the BUM spectral line consists of depolarized EM waves due to generation of turbulent plasma irregularities. The potential benefit of SEE measurement with FAIs and electron temperature provide insights for understanding the nonlinear wave and particle interaction in magnetized plasmas.

5 Acknowledgements

The authors would like to acknowledgment supports from M. A. McCarrick at HAARP and M. T. Rietveld and M. J. Kosch at EISCAT. The authors also appreciate J. M. Ruohoniemi, T. K. Yeoman and W. A. Bristow for SuperDAN HF radar support. H. Fu was supported by China National Science Foundation grant 41404122. The work at Virginia Tech was supported by the National Science Foundation. The work at the Naval Research Laboratory was sponsored by the NRL 6.1 Base program.

References

[1] B. Thidé, H. Kopka., and P. Stubbe, "Observations of stimulated scattering of a strong high-frequency radio wave in the ionosphere", *Physical Review Letters, 49*,21, 1982, pp. 1561-1564.

[2] T. B. Leyser, " Stimulated electromagnetic emissions by high-frequency electromagnetic pumping of the ionospheric plasma", *Space Science Reviews, 98*,3-4, 2001, pp. 223-328.

[3] T., B. Pedersen, E. Gustavsson, E. Mishin, E. Kendall, T. Mills, H. C. Carlson, and A. L. Snyder, "Creation of artificial ionospheric layers using high-power HF waves", *Geophysical Research Letters, 37*, 2, 2010.

[4] P. A. Bernhardt, C. A. Selcher, R. H. Lehmberg, S. Rodriguez, J. Thomason, M. McCarrick,, and G. Frazer,"Determination of the electron temperature in the modified ionosphere over HAARP using the HF pumped Stimulated Brillouin Scatter (SBS) emission lines", *Annales Geophysicae 27*, 12, 2009, pp. 4409–4427.

[5] L. Norin, T. B.Leyser, E. Nordblad, B. Thidé, and M. McCarrick, (2009), "Unprecedentedly strong and narrow electromagnetic emissions stimulated by high-frequency radio waves in the ionosphere", *Physical Review Letters*, *102*, 6, 2009, pp.065003, doi:10.1103/PhysRevLett.102.065003.

[6] P. A. Bernhardt, C. A. Selcher, R. H. Lehmberg, S. P. Rodriguez, J. F. Thomason, K. M. Groves, M. J. McCarrick, and G. J. Frazer(2010), Stimulated Brillouin Scatter in a magnetized ionospheric plasma, *Physical Review Letters*, *104*, 165004, 2010, pp.1-4.

[7] H. Fu, W. A. Scales, P. A. Bernhardt, A. Samimi, A. Mahmoudian, S. J. Briczinski, and M. J. McCarrick,"Stimulated Brillouin scatter and stimulated ion Bernstein scatter during electron gyroharmonic heating experiments", *Radio Science*, *48*, 2013, pp. 607-616.

[8] E. N. Sergeev, A. V. Shindin, S. M. Grach, G. M. Milikh, E. V. Mishin, P. A. Bernhardt, C. L. Siefring, S. J. Briczinski, and M. J. McCarrick, "Exploring HF-induced ionospheric turbulence by Doppler sounding and stimulated electromagnetic emissions at the High Frequency Active Auroral Research Program heating facility", *Radio Science*, *51*,7, 2016, pp.1118-1130, doi:10.1002/2015RS005936.

[9] W. A. Scales, "Some Recent Advances in Stimulated Radiation Investigations During Radiowave Heating of the Near Earth Space Environment", *Radiation Effects and Defects in Solids*, *171*, 1-2, 2016, pp.2-12, DOI: 10.1080/10420150.2016.1155586, 2016.

[10] H. Y. Fu, W. A. Scales, P. A. Bernhardt, S. J. Briczinski, M. J. Kosch, A. Senior, M. T. Rietveld, T. K. Yeoman, and J. M. Ruohoniemi , "Stimulated Brillouin Scattering During Electron Gyro-Harmonic Heating at EISCAT", *Annales Geophysicae*, *33*, 2015, pp.983-990.

[11] J. Huang, , and S. P. Kuo, " A generation mechanism for the downshifted peak in stimulated electromagnetic emission spectrum", *Journal of Geophysical Research: Space Physics* ,*100*,A11, 1995, pp.21433-21438.

[12] T. D. Carozzi, B. Thide, T. B. Leyser, G. Komrakov, V. Frolov, S. Grach and E. Sergeev, "Full polarimetry measurements of stimulated electromagnetic emissions: First results", *Journal of Geophysical Research: Space Physics* , *106*, 106, A10, 2011, pp.21395-21407.